Irrig Sci (2009) 28:35–50
DOI 10.1007/s00271-009-0179-7

REVIEW

# Evaluating eddy covariance cotton ET measurements in an advective environment with large weighing lysimeters

José Luis Chávez · Terry A. Howell · Karen S. Copeland

Received: 15 October 2008 / Accepted: 30 April 2009 / Published online: 3 September 2009


**Abstract** Eddy covariance (EC) systems are being used to assess the accuracy of remote sensing methods in mapping surface sensible and latent heat fluxes and evapotranspiration (ET) from local to regional scales, and in crop coefficient development. Therefore, the objective was to evaluate the accuracy of EC systems in measuring sensible heat (H) and latent heat (LE) fluxes. For this purpose, two EC systems were installed near large monolithic weighing lysimeters, on irrigated cotton fields in the Texas High Plains, during the months of June and July 2008. Sensible and latent heat fluxes were underestimated with an average error of about 30%. Most of the errors were from nocturnal measurements. Energy balance (EB) closure was 73.2–78.0% for daytime fluxes. Thus, daylight fluxes were adjusted for lack of EB closure using the Bowen ratio/preservation of energy principle, which improved the resulting EC heat flux agreement with lysimetric values. Further adjustments to EC-based ET included nighttime ET (composite) incorporation, and the use of 'heat flux source area' (footprint) functions to compensate ET when the footprint expanded beyond the crop field boundary. As a result, ET values remarkably matched lysimetric ET values, with a 'mean bias error ± root mean square error' of $-0.03 \pm 0.5$ mm day$^{-1}$ (or $-0.6 \pm 10.2\%$).

Communicated by S. Ortega-Farias.

J. L. Chávez (✉)
Department of Civil and Environmental Engineering,
Colorado State University, 1372 Campus Delivery,
Fort Collins, CO 80523-1372, USA
e-mail: jose.chavez@colostate.edu

T. A. Howell · K. S. Copeland
Conservation and Production Research Laboratory,
USDA-ARS, P.O. Drawer 10, Bushland, TX 79012, USA
e-mail: terry.howell@usda.ars.gov

K. S. Copeland
e-mail: kare.copeland@usda.ars.gov

## Introduction

Surface energy fluxes [net radiation ($R_n$), sensible heat flux ($H$), latent heat flux (LE), and soil heat flux ($G$)], all in W m$^{-2}$ units, can be measured fairly accurately at a given site over an extended period of time. For instance, lysimeters were used to measure water mass loss [therefore LE or crop/soil evapotranspiration (ET)] with high accuracy, according to Howell et al. (1995). They indicated that the lysimeter total measurement error was less than 1% in the range of water mass change of 0.05 mm (450 g) to 250 mm (2.25 Mg). The authors added that the lysimeter accuracy was sufficient to determine ET rates as small as 0.05 to 0.1 mm h$^{-1}$ over time periods of 30 min or greater. In terms of net radiometers' measurement accuracy (used to measure net radiation), Hipps (2003) indicated that the net radiometers error typically ranged between 5 and 10%, while soil heat flux measurements made with soil heat flux plates (SHFP) reported errors around 20–30%. However, a few point measurements are not enough for larger scales (local to regional) estimates of the surface energy fluxes and ET due to the surface heterogeneity. These spatially distributed fluxes are required in hydrology, agriculture, and weather forecasting.

To fill this need, remote sensing (RS) of land surface energy balance (EB) can potentially be and has been used to ultimately provide instantaneous estimates of LE or ET. These instantaneous LE estimates have been used in the prediction and monitoring of spatially distributed daily (24 h) crop water use/ET, irrigation scheduling, and in general hydrologic modeling (Boegh et al. 2004; Santos et al. 2008).

The different RS-based EB algorithms need to be validated in order to be routinely applied, with confidence and with known uncertainties, when estimating ET. In general, eddy covariance (EC) and weighing lysimeters are used for such validations because they directly measure the water consumed by crops and the evaporation from bare soils (Hipps and Kustas 2001; Shuttleworth 2007; Chávez et al. 2007) or by EB Bowen ratio (BR) or by soil water balance (both indirect methods). For instance, Boegh et al. (2004) incorporated RS data in hydrologic models as well as EC system ET estimates for calibration/evaluation of the models. Holifield et al. (2008) used EC flux stations to verify RS ET estimates. Kustas et al. (1994) used NOAA-11 AVHRR satellite imagery collected over the USDA-ARS Walnut Gulch Experimental Watershed in southeastern Arizona, during the MONSOON 90 field campaigns. During that study, they used an EB model that relies primarily on remotely sensed inputs to extrapolate ET estimates from one location containing near-surface meteorological data to other areas in the watershed. They extrapolated one time of day ET estimates to daytime averages using the evaporative fraction (EF) concept. Their model reportedly derived daytime average ET that compared reasonably well with local ground-based measurements made with EC EB systems.

Mu et al. (2007) used a network of 19 EC systems to validate a global RS-based ET algorithm using MODIS satellite imagery. Mecikalski et al. (1999) used EC systems to verify sensible and latent heat flux estimates from satellites as well. Similarly, Chávez et al. (2005) used a network of EC systems to validate high resolution airborne RS LE (ET) estimates over rainfed corn and soybean fields near Ames, IA; and over dense riparian vegetation (Salt Cedar, *Tamarix* spp.) in the middle Rio Grande river in New Mexico (Chávez and Neale 2003).

In addition, EC and BR systems were used in the study carried out by Kustas et al. (2005) and Suleiman and Crago (2004). They used daytime conservation of EF as $ET/R_n$ to extrapolate from hourly RS-derived ET to daytime ET. Suleiman and Crago (2004) reported a RMSE (root mean square error) between hourly predicted and measured LE of 30–50 W $m^{-2}$. The slope and $R^2$ for the zero-intercept linear regression between daytime estimated and measured LE ranged from 0.89 to 1.07 and 0.69 to 0.9, respectively.

Therefore, assessing the accuracy and limitations of EC systems, using precision lysimeters, is crucial for improving crop water management practices, since EC systems are used to validate/calibrate RS-based ET algorithms as well as in the development of crop coefficients (Malek and Bingham 1993). Most importantly, this evaluation is needed when agricultural fields (irrigated) are located in semiarid regions subjected to sensible heat advection from dry/hot fallow lands and natural eco-systems. Thus, the main objective of this paper was to assess the accuracy of EC systems in measuring ET over irrigated cotton fields in the advective environment of the Southern High Plains.

## Materials and methods

### Study area

This research was conducted during the 2008 cotton cropping season at the USDA-ARS, Conservation and Production Research Laboratory (CPRL), located at Bushland, TX. The geographic coordinates of the CPRL are 35°11′N, 102°06′W, and its elevation is 1,170 m above mean sea level. Soils in and around Bushland are classified as slowly permeable Pullman clay loam. The major crops in the region are corn, sorghum, winter wheat, and cotton. Wind direction is predominantly from the south/southwest direction. Annual average precipitation is about 562 mm. However, only 280 mm of precipitation occurs during the cotton growing season while about 670 mm of water are needed to grow cotton (New 2005), thus irrigation needs to provide about 390 mm of timely water for a successful cotton harvest. In addition, the long-term annual micro-climatological conditions indicate that the study area is subject to a very dry air and strong winds. Annual averages for air temperature, air water vapor pressure deficit, and horizontal wind speed are 14°C, 0.3 kPa, and 4.9 m $s^{-1}$, respectively.

### Weighing lysimeter

Two precision weighing lysimeters (Marek et al. 1988), 3 × 3 × 2.3 m, were used to directly measure cotton ET. Each lysimeter contained a monolithic Pullman clay loam soil core. The lysimeters were located at the centers of the north and south experimental field [4.7 ha each, i.e., 210 m wide (East–West) × 225 m long (North–South)]. The change in lysimeter mass was measured by load cell (model SM-50, Interface, Scottsdale, AZ) and recorded by a datalogger (model CR7-X, Campbell Scientific, Inc., Logan, UT). The signal was sampled at 0.17-Hz (i.e., 1 sample every 6 s) frequency. The high frequency load cell signal was averaged for 5 min and composited to 15-min means. The lysimeters were calibrated using techniques as explained in Howell et al. (1995). The lysimeter mass measurement accuracy in water depth equivalent was 0.01 mm, as indicated by the RMSE of calibration.

Each lysimeter field was equipped with one net radiometer (model REBS Q*7.1, REBS, Radiation and Energy Balance Systems, Bellevue, WA), four SHFP (model

HFT-3, REBS, Radiation and Energy Balance Systems, Bellevue, WA), and four pairs of soil thermocouples (model TMTSS-125G-6, Omega Engineering, Inc., Stamford, CT), for measuring net radiation, soil heat flux, and temperature for soil heat storage, respectively. The net radiometer was installed at about 1.5 m above the ground in the center of the N lysimeter side facing to the S. SHFP were installed at 0.08-m depth at four locations within and between the crop rows. Soil thermocouple pairs were wired in parallel to average the temperature and installed at 0.02 and 0.07 m depths close to the SHFP locations.

In addition, each lysimeter was equipped with an array of radiation instruments, air temperature/relative humidity sensor, and an anemometer. Besides the Q*7.1 net radiometer, a net short-wave radiation (model CMA 11, Kipp and Zonen USA, Bohemia, NY), and a reflected photon flux density (photosynthetically active radiation, PAR, model LI-190 Quantum Sensor, LI-COR, Inc., Lincoln, NE) shielded to a 30° NADIR FOV were also installed at the lysimeter location. Other instruments included in the array were a couple of infrared thermometers (model IRT/c, Exergen Corp., Watertown, MA), which were mounted to view approximately at a 60° zenith angle and an azimuth toward the Southwest at 45° from due S. The N lysimeter had a net pyrgeometer (model CGR 4, Kipp and Zonen USA, Bohemia, NY) to also measure net long-wave radiation. A temperature/relative humidity was measured with a sensor (model HMP45C, Campbell Scientific, Inc., Logan, UT manufactured by Vaisala, Inc., Woburn, MA) mounted in a Gill shield (model 41003-5 10-Plate Gill radiation shield manufactured by R.M. Young, Traverse City, MI) at 2 m above the ground. Wind speed was measured by an anemometer (model 03101-L R.M. Young wind sentry anemometer, Campbell Scientific, Inc., Logan, UT manufactured by R.M. Young, Traverse City, MI) at 2 m above the ground. All lysimeter water mass change and ancillary meteorological data (at the lysimeter site) were recorded with a data logger (model CR-7X, Campbell Scientific, Inc., Logan, UT).

## Eddy covariance

Eddy covariance is based on the direct turbulent measurements of the product of vertical velocity fluctuations ($w'$) and a scalar (e.g., air temperature, water vapor, carbon dioxide, horizontal wind speed, etc.) concentration fluctuation ($c'$) producing a direct estimate of $H$, LE, $CO_2$, and momentum (shear forces) fluxes, under the assumption that the mean vertical velocity is zero. This implies that if turbulence is treated as a set of fluctuations about a mean value, which is called Reynolds averaging, then the value of any variable at a given time is the sum of a temporal mean (over some time period) plus an instantaneous deviation. EC principles and history can be found in Hipps and Kustas (2001) and Shuttleworth (2007), respectively. Burba and Anderson (2007) provide an on-line guidelines for EC method installation, use, maintenance, data post-processing, etc.

Two identical EC systems were installed on the lysimeter fields, each about 15 m North–East of the lysimeter box, i.e., downwind of the predominant wind direction. Each EC system consisted of a fast response 3D sonic anemometer (model CSAT3, Campbell Scientific Inc., Logan, UT), a fast response open path infrared gas ($H_2O$ and $CO_2$) analyzer (model LI-7500, LI-COR Inc., Lincoln, NE), a fine wire thermocouple (model FW05, Campbell Scientific Inc., Logan, UT), an air temperature/humidity sensor (model HMP45C, Vaisala Inc., Woburn, MA), and a micrologger (model CR3000, Campbell Scientific Inc., Logan, UT). A constant air density measured as the mean for each 15-min period was used (model CS106, Vaisala PTB110 barometer, Campbell Scientific, Logan, UT) to compute the flux terms.

The EC system measured turbulent fluxes at a high frequency of 20 Hz (20 samples per second) and 15-min average LE and $H$ fluxes were computed. Both EC systems were installed at a 2.5 m height above ground level and were kept at the same height during the entire experiment. The cotton canopy height had reached 0.20 m by 26 June and 0.64 m by 28 July 2008. The CSAT3 sensor was oriented toward the predominant wind direction, with an azimuth angle of 225° from true North. The magnetic declination angle was taken into account in the EC program.

The raw high frequency data (20 samples per second) were corrected for effects of density fluctuations induced by heat fluxes on the measurement of eddy fluxes of water vapor using the LI-7500. This correction is called the WPL correction (Webb et al. 1980), i.e., the Webb, Pearman and Leuning correction. Leuning (2007) provides a detailed description of the principles and theory of the WPL correction. According to Mauder and Foken (2006), the WPL correction is a very important correction procedure since it can correct scalar fluxes up to 50%. On the other hand, no corrections were made on the raw data to account for sensor separation because the CSAT3D and LI-7500 sensors were installed within specification, i.e., 10 cm form center to center, and the cotton field was mostly homogeneous (small spatial variability of cotton leave area index and crop height, as per the standard deviation values derived from RS imagery). Moore (1986) indicated that when close to proper sensor separation is achieved, coordinate rotation corrections may result in flux adjustments of less than 3%. Thus, considering the previous statement and the fact that the terrain was practically flat, with minimum slope in the East–West direction, neither coordinate transformations were performed nor data de-trending was pursued because the 15-min averaging period was considered short for non-stationarity presence.

Heat fluxes were collected during the following days of the year (DOY), in June and July of 2008, for the EC system located in the North lysimeter field (denominated EC1), data were acquired from 24 days: 158, 159, 163, 164, 166, 174, 175, 178, 179, 182, 183, 184, 187, 188, 189, 193, 194, 195, 200, 203, 205, 206, 208, and 209. And for the EC system located on the South lysimeter field (EC2), data from 18 days were acquired: DOY 174, 175, 178, 179, 182, 183, 184, 187, 188, 189, 193, 194, 200, 203, 205, 206, 208, and 209. All other days during the months of June and July were discarded because they were either irrigation or rainy days. System EC2 started acquiring data later in June, i.e., on DOY 174 and not on DOY 158 as in the EC1 case.

The location of the EC stations, lysimeters, and grass reference weather station is displayed in Fig. 1. While Fig. 2a displays a picture of the SE lysimeter box showing the location of the SE EC system (background, upper left portion), Fig. 2b a close up picture of the SE EC system, and Fig. 2c shows the grass reference weather station.

### Latent heat flux conversion into ET rates

Latent heat fluxes (W m$^{-2}$) were converted into an equivalent water depth or 15-min ET rates expressed as mm h$^{-1}$ in order to properly compare with the lysimetric measured ET values.

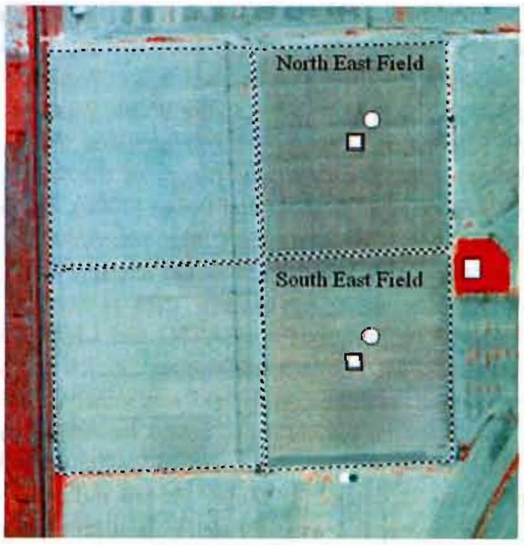


**Fig. 1** Three-band false color composite reflectance image, for day of year (DOY) 178, showing location of eddy covariance stations (*circles*), lysimeters (*bevel square*) and grass reference weather station (*rectangle*)

LE was converted into ET as follows:

$$\mathrm{ET} = \left(\frac{3{,}600 \times \mathrm{LE}}{\lambda_{\mathrm{LE}} \times \rho_{\mathrm{w}}}\right) \quad (1)$$

where ET is evapotranspiration (mm h$^{-1}$) converted from EC measured LE (W m$^{-2}$). $\lambda_{\mathrm{LE}}$ the latent heat of vaporization (MJ kg$^{-1}$), equal to (2.501–0.00236 $T_a$), being $T_a$ in °C units, and $\rho_w$ is water density ($\sim$1 Mg m$^{-3}$). The 3,600 number is a time conversion of s h$^{-1}$.

### Heat flux source area (footprint) models

In an effort to understand and define the upwind area that contributes with heat fluxes to EC (or BR) system, 'flux area source' or footprint (FTP) models have been developed. The footprint models determine what area upwind of towers is contributing with heat fluxes to the sensors, as well as the relative weight of each particular cell (sub-area) inside the footprint limits. Different footprint models have been proposed, 1D and 2D models. These models are the analytical solution to the diffusion–dispersion–advection equation (Horst and Weil 1992, 1994). Other models are Lagrangian (Leclerc and Thurtell 1990). Studies using these models were able to prove that depending on the height of the vegetation, height of the instrumentation, wind speed, wind direction standard deviation, and atmospheric stability condition, the shape and length of the footprint would change upwind of the instruments. In addition, the FTP model indicates the relative weights (magnitude of contribution) in each individual cell/area inside the footprint. Areas very close to the station contribute less to the total flux sensed by the instrument, areas further away (upwind) increasingly contribute more, up to a point where a peak is reached, thereafter the contribution decreases rapidly further upwind from the station (Verma 1998). Similar behavior describes the crosswind flux distribution detected by the instruments.

Gash (1986) footprint model is a structurally simple solution to the analytical-diffusion equation, which assumes neutral atmospheric conditions, for estimating the fetch for which above-canopy measurements are representative. Gash's equation has been shown to be capable of satisfactorily approximating the numerical simulation over a wide range of heights, zero displacements and roughness lengths. Gash's equation follows:

$$\rho(x,z) = \frac{Q_{\mathrm{L}}}{\kappa u_* x}\, \mathrm{e}^{-Uz/\kappa u_* x} \quad (2)$$

where, $\rho(x, z)$ is the gas or water vapor concentration resulting from an infinite crosswind line source located at an upwind distance, $x$, in a uniform wind field ($U$ and $\kappa$ are constants), $Q_{\mathrm{L}}$ is source strength per unit length, $\kappa$ is the von Karman constant, equal to 0.41, $u_*$ is the friction velocity (m s$^{-1}$), $z$ is the height (m) above the zero

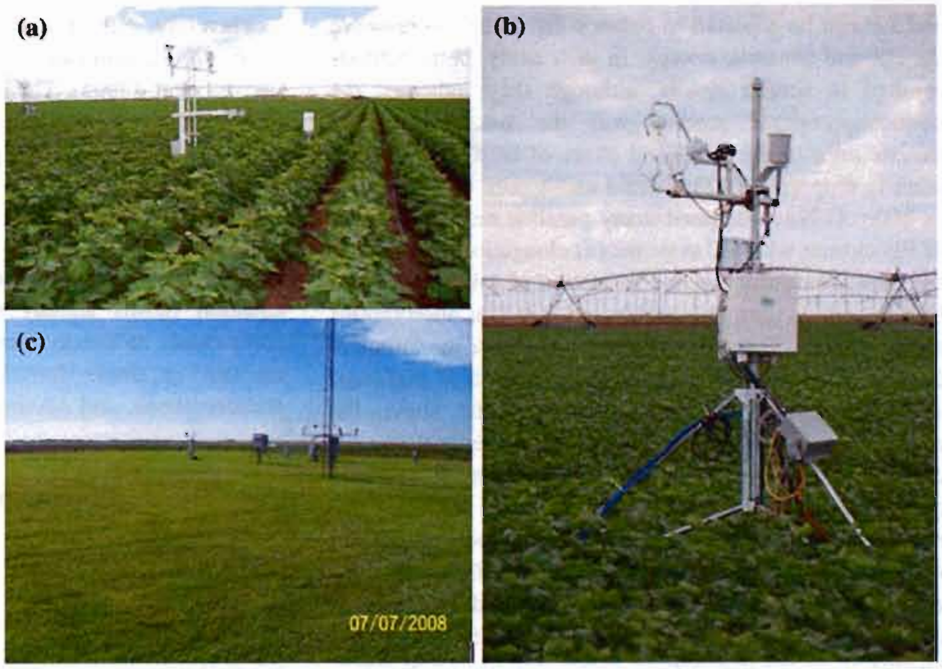


**Fig. 2** Southeast lysimeter (SE) box (**a**) showing the eddy covariance (EC) system on the *upper left* corner (background), SE EC system (**b**), and grass reference weather station (**c**)

displacement ($d$, m), and $U$ is the assumed constant wind speed (m $s^{-1}$), defined as the average wind speed between the surface and observation height, $z$.

Thus, removing $Q_L$ from the equation above one obtains the relative contribution at a given upwind distance form the instrument/tower location.

Kaharabata et al. (1997) presented a 2D footprint model that based on the basic concepts summarized by Horst and Weil (1992, 1994). Kaharabata et al. (1997) 2D footprint formulation used the actual crosswind Gaussian distribution instead of the crosswind-integrated flux distribution function. This resulted in the generation of heat flux weights in the $x$ and $y$ direction, upwind of the measuring instrument. The new function was expressed as:

$$F(x, y, Z_m) = \frac{u_* k}{\Psi_h\left(\frac{Z_m}{L_{M\_o}}\right)} \frac{s Z_m^s}{(B\sigma_z)^s} \frac{e^{-\left(\frac{y^2}{2\sigma_y^2}\right)}}{\sqrt{2\pi}\sigma_y} \frac{e^{-\left(\frac{Z_m}{B\sigma_z}\right)^s}}{A\sigma_z U(x)} \quad (3)$$

where, $F(x, y, Z_m)$ is the footprint or source weight function, $x$ is the upwind distance from the tower or sensor location, $y$ is the crosswind distance from the axis parallel to the wind direction ($x$), m, s is a shape exponent 1 for unstable conditions, 2 for very stable conditions, and 1.3–1.5 for neutral conditions. Table 4 in Chávez et al. (2005) shows the different equations/variables involved in the footprint function $F(x, y, Z_m)$ described above.

FSAM (Flux Source Area Model) by Schmid (1994) based on the Horst and Weil (1992) model (coded in Fortran) generates the FTP weights for the source area and the approximate dimensions of the FTP area for an area that contributes up to 90% of the sensed fluxes by the instrumentation. It includes the crosswind-integrated flux as Horst and Weil (1992, 1994):

$$F(x, y, Z_m) = D_y(x, y)\overline{F^y}(x, Z_m) \quad (4)$$

where $F(x, y, Z_m)$ is the footprint weight function, $D_y(x, y)$ is the crosswind distribution function, and $\overline{F^y}(x, Z_m)$ is the crosswind integrated function.

## Adjustment of turbulent fluxes

Twine et al. (2000) reported EC EB closures ranging from 70 to 90%. These authors suggested that when the available energy (AE = $R_n$ – G) measurement errors are known, EC measurements of sensible and latent heat fluxes should be adjusted for closure maintaining the BR. In their study, sunrise to sunset average flux closure was usually greater than for each 30 min values throughout the day. In this same study, extensive measurements from the Southern Great Plains 1997 Hydrology Experiment in Oklahoma were used to investigate closure of the EB (Twine et al. 2000). The authors reported that relative uncertainties associated with measurements of $G$ can be large because the area of measurement is several orders of magnitude smaller than the averaging area of EC measurements. They indicated that one option of forcing closure is to assume that $H$ is accurately measured, and solve LE as a residual to the EB equation, using only daytime fluxes. They referred to this method as the 'residual-LE closure.' Another option, they indicated, was to assume that the BR was correctly measured by the EC system so that individual values of $H$

and LE can be adjusted to balance Eq. 5, i.e., to preserve the BR and conserve energy. In their study, both methods resulted in similar results, although they indicated the correct/appropriate method was the BR, because of uncertainties in the value and phase of $G$. This last statement is supported by Fitzjarrald and Moore (1994).

Mahrt (1998) discussed many possible reasons for lack of EB closure with EC systems: (a) elongation of eddies in the downwind direction and formation of roll vortices can lead to serious sampling problems for in situ observations such as towers. The roll vortices can modulate the turbulent flux on a timescale that is longer compared to the usual averaging time, (b) tower fluxes must be above the roughness sub-layer, which might be considerably above a crop canopy, i.e., high flux divergence arising from transport of fluxes from multiple surfaces, (c) if fluxes are measured too close to the surface where the transporting eddies are small and the vertical velocity fluctuation are weak (height of the instrumentation limited by the fetch requirements), the instrumentation may not completely resolve all of the transporting eddies due to loss of small-scale flux associated with path averaging or instrument response time, (d) with weak wind speeds, the tilt correction to the sonic exerts a much stronger influence on the fluxes than at moderate and strong wind speeds (with weak winds, the sample size of the large eddies may be too small and to increase the sample size, tower fluxes are usually averaged over a longer period such as 30 min which usually reduces the random flux error but may capture additional non-stationarity (trends), (e) non-stationarity of measured time series over the chosen averaging period resulting in missing covariance data from very low frequency fluctuations (eddies), (f) turbulent dispersive fluxes arising from organized planetary boundary layer circulation that may have preferred locations so that the mean vertical velocities at an instrument location may be systematically different from zero giving rise to a mean vertical advective flux, and (g) measurement errors related to sensor separation, frequency response, alignment problems, and interference from tower or instrument mounting structures.

According to Shuttleworth (2007), systematic underestimation of surface fluxes almost always occurs when using the EC technique, especially at night. When measuring evaporation, such underestimation is troublesome; although the extent of loss during the day can be estimated (and perhaps corrected) by calculating the recovery ratio for surface energy fluxes relative to a measured energy budget. Errors in compensating nighttime ET are small since nighttime ET is small. Todd et al. (2000) found out that the difference between ET estimated with a BR system and lysimetric data averaged 5–15% during the daytime and 25–45% at night.

Therefore, EB closure was 'forced' following Twine et al. (2000) rationale and similarly as implemented in Chávez et al. (2005). The derivation of the amount of heat flux to add to $H$ and LE, to compensate for lack of EB closure, following the EB preservation of energy concept follows:

$$R_n = H + \mathrm{LE} + G. \quad (5)$$

Equation 5 represents the EB for land surface simplified equation (terms already defined), after ignoring small components as energy stored in the plant biomass (only relevant in dense forests), energy used in the plant photosynthesis, and advected energy. Thus,

$$D = (R_n - G) - (H + \mathrm{LE}) \quad (6)$$

where $D$ is the EB discrepancy (W $m^{-2}$). Also $D$ can be written as:

$$D = \Delta H + \Delta\mathrm{LE}. \quad (7)$$

Considering the definition of the BR as:

$$\mathrm{BR} = H/\mathrm{LE} \quad (8)$$

where the BR value used to correct every 15-min heat flux was the around-noon average value (from 10:00 a.m. to 2:00 p.m. CST). This average BR was adopted since it is more stable/constant during this period. Chávez et al. (2005) obtained good results utilizing this procedure. They discussed the rationale behind the adoption of the around-noon BR average to adjust EC heat fluxes measured through out the entire day.

Next, $H$ and LE discrepancies of Eq. 7 are added to Eq. 8 keeping the BR:

$$\mathrm{BR} = (H + \Delta H)/(\mathrm{LE} + \Delta\mathrm{LE}). \quad (9)$$

Then ΔLE can be expressed as:

$$\Delta\mathrm{LE} = [(H + \Delta H)/\mathrm{BR}] - \mathrm{LE}. \quad (10)$$

Further incorporating Eq. 7, solved for $\Delta H$, in Eq. 10:

$$\Delta\mathrm{LE} = [(H + D - \Delta\mathrm{LE})/\mathrm{BR}] - \mathrm{LE}. \quad (11)$$

Doing some arithmetic and solving for ΔLE, inserting Eq. 8 we obtain:

$$\Delta\mathrm{LE} = D/(1 + \mathrm{BR}). \quad (12)$$

From Eqs. 12 and 7, $\Delta H$ is:

$$\Delta H = D \times (1 - 1/(1 + \mathrm{BR})) \text{ or simply } \Delta H = D - \Delta\mathrm{LE}. \quad (13)$$

Therefore, the amount of heat flux to add to (EC) measured $H$ and LE, to compensate for lack of EB closure, is $\Delta H$ and ΔLE, respectively. These corrections were performed on day light fluxes.

However, computing diel ET values using only daytime LE fluxes does not yield the total daily ET amount because nighttime ET could be 7–10% of the whole day ET in the Southern High Plains (Tolk et al. 2006a, b). The entire day ET is really the value needed to quantify the correct amount of soil water used by the crop in order to elaborate an appropriate soil water balance for irrigation scheduling, for instance. Hence, for this purpose we need to consider the amount of ET occurring during the nighttime hours. Therefore, to account for nocturnal ET the following procedure was followed: (a) the EC-based daytime ET fraction was computed by dividing the average EC daytime ET by the average EC 24 h ET (both EB closure adjusted), then, (b) the nighttime ET fraction was obtained from subtracting the daytime ET fraction from one (1), finally, (c) the diel ET amount was calculated as 'daytime ET + (daytime ET × nighttime ET fraction),' this computation was called 'composite' ET, i.e., daylight plus nighttime ET.

### Statistical analysis

Comparisons between lysimeter ET-measured values and EC-measured/adjusted ET values were performed by computing the mean bias error (MBE, Eq. 14) or average error, the RMSE (Eq. 15) or error standard deviation in mm day$^{-1}$ and in percent (% of the mean), and through a linear regression analysis based on least squares method for comparison of fitted equation slope, intercept and goodness of fit values.

$$\mathrm{MBE} = \frac{1}{n}\sum_{i=1}^{n}\left[X(M)_i - X(O)_i\right] \tag{14}$$

where $n$ is the number of pairs compared, $X(M)_i$ the 'estimated'/measured EC-based ET value and $X(O)_i$ is the reference/observed value (lysimeter-based ET). A negative MBE means that the EC system under scored the reference value.

$$\mathrm{RMSE} = \sqrt{\frac{1}{n-1}\sum_{i=1}^{n}\left\{\left[X(M)_i - X(O)_i\right] - \mathrm{MBE}\right\}^2}. \tag{15}$$

Equation 15 removes the bias effect of the estimator ($M$) over the mean squared error (MSE); as described in Birks et al. (1990). Therefore, the RMSE becomes the standard deviation of the MBE.

## Results and discussion

### Sensible heat flux evaluation

First the EC sensible heat flux measurements were evaluated comparing average diel 15-min values with $H$ computed as a residual from the EB at the North lysimeter site. Results show that EC1 under quantified $H$ by 28.2% while EC2 under quantified $H$ by 45.0%. Both EC systems showed a large RMSE in measured values, mainly on very low and/or negative values, i.e., when advective conditions prevailed. In this case, the atmospheric conditions were such that the average daily air temperature, relative humidity, wind speed and grass reference ET range were 22–27°C, 50–70%, 5–6.5 m s$^{-1}$, and 8–12 mm day$^{-1}$, respectively. The underestimation persisted in most of the days included in the analysis for both sites.

Considering that, in general, most negative and low $H$ values occurred at nighttime, when the atmospheric condition was predominantly stable or near neutral conditions, another analysis was performed using only daytime values ($\sim$14 h) to avoid the effect of nighttime $H$ fluxes in the computation of daily $H$ values. In this new analysis, for both cases EC1 and EC2, the underestimation decreased but still was large, 35 and 37%, respectively, with an error spread of 33.2 and 26.9%, respectively. Complete error quantification in energy units and percent, as well as least square linear regression parameters, can be found in Table 1.

The underestimation of $H$ is reflected in the low EB closure, $\{[(\mathrm{LE} + H)/(R_n - G)] \times 100\}$, observed on the EC $H$ and LE measured values. In average, EB closure for the daily (including day and night) average heat fluxes was 53.9% at site EC1 (standard deviation or RMSE of 3.9%), and 72.5% at site EC2 (RMSE of 5.6%). For the daytime fluxes, the average EB closure was 78.0% (RMSE of 5.1%), higher than the 24 h closure of site EC1, while it was marginally higher for site EC2, 73.2% with an RMSE of 5.9%.

The lack of EB closure of EC system is commonly reported in the literature. For instance, during the FIFE [First International (Satellite Land Surface Climatology Project) Field Experiment] research over grassland, Fritschen et al. (1992) found out that an EC system EB closure averaged 84% during a period of 3 days. Typical errors for EC EB terms were reported by Weaver (1990), Field et al. (1994), and Hipps (2003) to fall between 15 and 20% for $H$, 15–20% for LE, 5–10% for $R_n$, and 20–30% for $G$. Wilson et al. (2002) found an average 80% closure, or a 20% imbalance, on a study using 22 EC sites and 50 site-years in contrasting ecosystems and climates (Mediterranean, temperate, and arctic). Chávez et al. (2005), in a study involving a network of EC systems on rainfed corn and soybean fields, found that the EC systems EB closure in average ranged from 57 to 109%, being the under prediction of $H$ and LE the norm under highly unstable atmospheric conditions [i.e., $H$ very large and positive (away from the surface), because the aerodynamic temperature (within canopy) was much greater than the air temperature at screen height)]. In yet another study, Oncley

**Table 1** Comparison of EC diel average (avg) and 14 h avg *H* with residual *H* values from the EB at the lysimeter site

| Site | *H* analysis | MBE (W m$^{-2}$) | MBE (%) | RMSE (W m$^{-2}$) | RMSE (%) | Slope | Intercept (W m$^{-2}$) | $R^2$ |
|---|---|---|---|---|---|---|---|---|
| EC1 | 24 h avg *H* | 1.44 | −28.2 | 21.0 | 77.3 | 0.65 | −18.7 | 0.88 |
| EC2 | 24 h avg *H* | 23.6 | 58.2 | 27.4 | 42.1 | 0.56 | 16.1 | 0.88 |
| EC1 | 14 h avg *H* | −30.9 | −35.0 | 38.3 | 33.2 | 0.62 | 12.8 | 0.93 |
| EC2 | 14 h avg *H* | −38.4 | −37.0 | 23.6 | 26.9 | 0.72 | −0.96 | 0.88 |

*MBE* mean bias error, *RMSE* root mean squared error, $R^2$ coefficient of determination, *EC1* eddy covariance system 1, *EC2* eddy covariance system 2, *H* sensible heat flux, *EB* energy balance

**Table 2** Descriptive statistics of LE and *H* percent closure adjustments

| System | Heat flux | Average (%) | SD (%) | Max. (%) | Min. (%) | Median (%) |
|---|---|---|---|---|---|---|
| EC1 | LE | 74.2 | 13.6 | 120.6 | 47.5 | 73.7 |
| EC1 | *H* | 139.9 | 208.2 | 928.9 | −38.4 | 100.6 |
| EC2 | LE | 33.6 | 7.8 | 96.2 | 22.7 | 31.7 |
| EC2 | *H* | 32.9 | 45.2 | 96.2 | −89.8 | 43.7 |

*LE* latent heat flux, *H* sensible heat flux, SD standard deviation, *Max.* maximum value (%), *Min* minimum value (%), *EC1* eddy covariance system 1, *EC2* eddy covariance system 2

**Table 3** Descriptive statistics of daytime only LE and *H* percent closure adjustments

| System | Heat flux | Average (%) | SD (%) | Max. (%) | Min. (%) | Median (%) |
|---|---|---|---|---|---|---|
| EC1 | LE | 26.2 | 7.4 | 37.7 | 15.0 | 27.0 |
| EC1 | *H* | 36.4 | 23.4 | 91.1 | −22.3 | 38.7 |
| EC2 | LE | 35.6 | 10.0 | 56.3 | 19.2 | 34.7 |
| EC2 | *H* | 45.7 | 15.8 | 73.0 | 20.2 | 48.7 |

*LE* latent heat flux, *H* sensible heat flux, *SD* standard deviation, *Max.* maximum value (%), *Min* minimum value (%), *EC1* eddy covariance system 1, *EC2* eddy covariance system 2

et al. (2000) reported a lack of EC system EB closure of about 20%.

For the EB closure of heat fluxes derived from 15-min values averaged during the entire day, the adjustment for *H* was 139.9% for site EC1 and 32.9% for site EC2; while LE was adjusted an average 74.2% at site EC1 and 32.9% at EC2. More statistics showing the standard deviation (SD), maximum (max.), minimum (min.), and median (median) values can be found in Table 2.

Similar analysis of percent of EB closure adjustments for *H* and LE, as shown in Table 2, was performed for heat fluxes derived from daytime (~14 h) only 15-min values. Results showed that the adjustment for *H* was 36.4% for site EC1 and 45.7% for site EC2; while LE was adjusted in average 26.2% at site EC1 and 35.6% at EC2 (Table 3). Much lower EB closure adjustments occurred during daytime, which shows that at nighttime the EC system has difficulties measuring accurately scalar fluxes under the environmental conditions of the experiment.

Therefore, after forcing EB closure on EC-based *H* values, for both values obtained averaging 15-m measurements for the entire day and only those values during daytime, we observed that the EC-based *H* error decreased in both cases when compared with residual *H* values derived from lysimeters EB measurements. However, lower MBE and RMSE values can be observed for daytime *H* fluxes; where the correlation with residual *H* (lysimeter derived) was much better, the correlation slope was closer to 1.0, *Y*-axis intercept closer to zero and the coefficient of determination was slightly better (0.94 for EC1, and 0.92 for EC2) (Table 4). These results indicate that nighttime sensible heat fluxes are not accurately measured by the EC systems, most probably for lack of sufficient turbulence (eddies), stable to neutral atmospheric condition, and due to uncertainties in the nocturnal available energy measurements and advection.

Furthermore, most of the errors occurred on very small and/or negative *H* values. Thus, considering only *H* values greater than 50 W m$^{-2}$, diel average *H* error statistics for site EC1 were −1.6 W m$^{-2}$ (−26%) and RMSE of 18.1 W m$^{-2}$ (18.5%). In the case of site EC2, errors in *H* values were 11.2 W m$^{-2}$ (19.4%) and RMSE of 15.3 W m$^{-2}$ (27.9%). In addition, considering only *H* values averaged during daytime (period of hours with sunlight), *H* MBE for EC1 were −9.9 W m$^{-2}$ (or −4.6%) with a corresponding RMSE of 23.7 W m$^{-2}$ (or 15.1%). For site EC2, *H* errors were MBE of 1.6 W m$^{-2}$ (or 1.3%) and RMSE of 19.8 W m$^{-2}$ (or 13.2%). Thus, for daytime *H*, EC errors were considerably lower and comparable in magnitude to measurement errors inherent for net radiation or soil heat flux for example.

Consequently, these results are evidence that the EC systems used in this experiment, even though initially considerably underestimated the sensible heat flux, can be adjusted to close the EB using noon average EC-derived BR values and outcome adjusted *H* (daytime) values

Table 4 Comparison of closured 'forced' diel EC-based 24 and 14 h average (avg) *H* with lysimeter values

| Site | *H* analysis | MBE (W $m^{-2}$) | MBE (%) | RMSE (W $m^{-2}$) | RMSE (%) | Slope | Intercept (W $m^{-2}$) | $R^2$ |
|---|---|---|---|---|---|---|---|---|
| EC1 | 24 h avg *H* | −6.5 | −24.7 | 20.7 | 58.8 | 1.19 | −25.1 | 0.91 |
| EC2 | 24 h avg *H* | 17.7 | −11.1 | 18.3 | 53.3 | 0.79 | 26.0 | 0.92 |
| EC1 | 14 h avg *H* | 1.2 | −13.1 | 25.8 | 47.2 | 0.82 | 19.3 | 0.94 |
| EC2 | 14 h avg *H* | −2.6 | −9.9 | 20.7 | 36.8 | 0.99 | 1.2 | 0.92 |

*MBE* mean bias error, *RMSE* root mean squared error, $R^2$ coefficient of determination, *EC1* eddy covariance system 1, *EC2* eddy covariance system 2, *H* sensible heat flux

similar in magnitude (equal in phase) to true *H*, i.e., to residual *H* derived from measured LE (lysimeter), $R_n$, and *G* at the lysimeter sites.

## EC ET measurement evaluation

Initially, each 15-min ET value measured throughout the day by the EC systems was compared with the corresponding ET values measured by the lysimeters (NE and SE). Large under prediction of ET occurred on both sites, i.e., the MBE was −30% (RMSE of 59.1%) for EC1 and −38% (RMSE of 51.6%) for EC2, respectively. Table 5 details the ET errors in mm $h^{-1}$, percent, and the corresponding correlation parameters for both EC systems and for ET including/excluding EB closure adjustments. Also, Fig. 3 plots the daily progress of ET rates during DOY 194 to illustrate the large difference between EC and lysimeter measured ET rates; while Fig. 4 graphically depicts the percent EC-based ET errors, which are much larger during nighttime.

EB closure was 53.9% in average for EC1 (SD 3.9%) and 72.5% for EC2 (SD 5.6%) (Table 2). One of the reasons for a poor EB closure may be due to a different process, than the AE, that controlled canopy evaporation at night. For instance, Baldocchi (1994) indicated that nocturnal evaporation flux densities measured over the closed wheat crop were independent of available energy, and instead were a function of vapor pressure deficit and wind speed, i.e., surface aerodynamic conditions. Also, that the evaporation densities measured over the sparse crop were weakly dependent on AE (Baldocchi 1994).

EB closure was forced on each 15-min ET data, for the entire daily dataset, as indicated in the "Sensible heat flux evaluation". Results produced a slight improvement on the agreement between EC-based ET and lysimeter values (Table 5). The MBE was reduced from −30 to −23.9% for EC1, while its RMSE increased about 1%, from 59 to 60%, i.e., the large scatter remained although the main concentration of points moved closer to the 1:1 line. Also, note the increment in the correlation slope value (Table 5).

Following similar rationale as in the *H* case, LE values were analyzed averaging the 15-min data for a 24-h period (entire day) and only using daylight (~14 h) data to mainly eliminate any potential instrumentation (EC, Lysimeter) synchronization and random errors, and nocturnal data noise, respectively. The conversion of daytime average LE fluxes into ET rates is detailed in "Appendix".

Hence, for the 15-min LE data averaged over a 24-h period, the underestimation of ET for EC1 increased from −30 to −41.4%; although the RMSE substantially decreased from 59.1 to only 12.3%, again when average diel 15-min LE values were used in the analysis (Table 6; Fig. 5). In the case of EC2 site, the scatter decreased considerably with a RMSE of only 7.4%. After EB closure, the mean errors decreased even further to only 1.0 and 12.0% for EC1 and EC2, with a RMSE of 19.3 and 10.1%, respectively (Table 6). In terms of the linear correlation, both EC sites ET values better approached the 1:1 line (see slope column in Table 6; Fig. 5).

Now in the case of the daytime ET analysis, when no EB adjustments were done, the average error was reduced from −41.4 to −28.8% for EC1 and from −34.1 to −26.0% for EC2, respectively, in relation to the EC ET errors when computed from averaging LE in a 24-h period. In contrast, their respective RMSE basically remained unchanged

Table 5 Comparison of EC-based ET with lysimetric ET using each 15-min data

| Site | ET analysis | MBE (mm $h^{-1}$) | MBE (%) | RMSE (mm $h^{-1}$) | RMSE (%) | Slope | Intercept (mm $h^{-1}$) | $R^2$ |
|---|---|---|---|---|---|---|---|---|
| EC1 | No EB adjustment | −0.12 | −30.0 | 0.16 | 59.1 | 0.575 | 0.009 | 0.75 |
| EC2 | No EB adjustment | −0.10 | −38.0 | 0.11 | 51.6 | 0.633 | 0.004 | 0.88 |
| EC1 | EB closure | −0.08 | −23.9 | 0.14 | 60.2 | 0.692 | 0.010 | 0.75 |
| EC2 | EB closure | −0.05 | −22.0 | 0.19 | 78.9 | 0.868 | −0.012 | 0.87 |

*ET* evapotranspiration, *MBE* mean bias error, *RMSE* root mean squared error, $R^2$ coefficient of determination, *EC1* eddy covariance system 1, *EC2* eddy covariance system 2, and *EB* energy balance

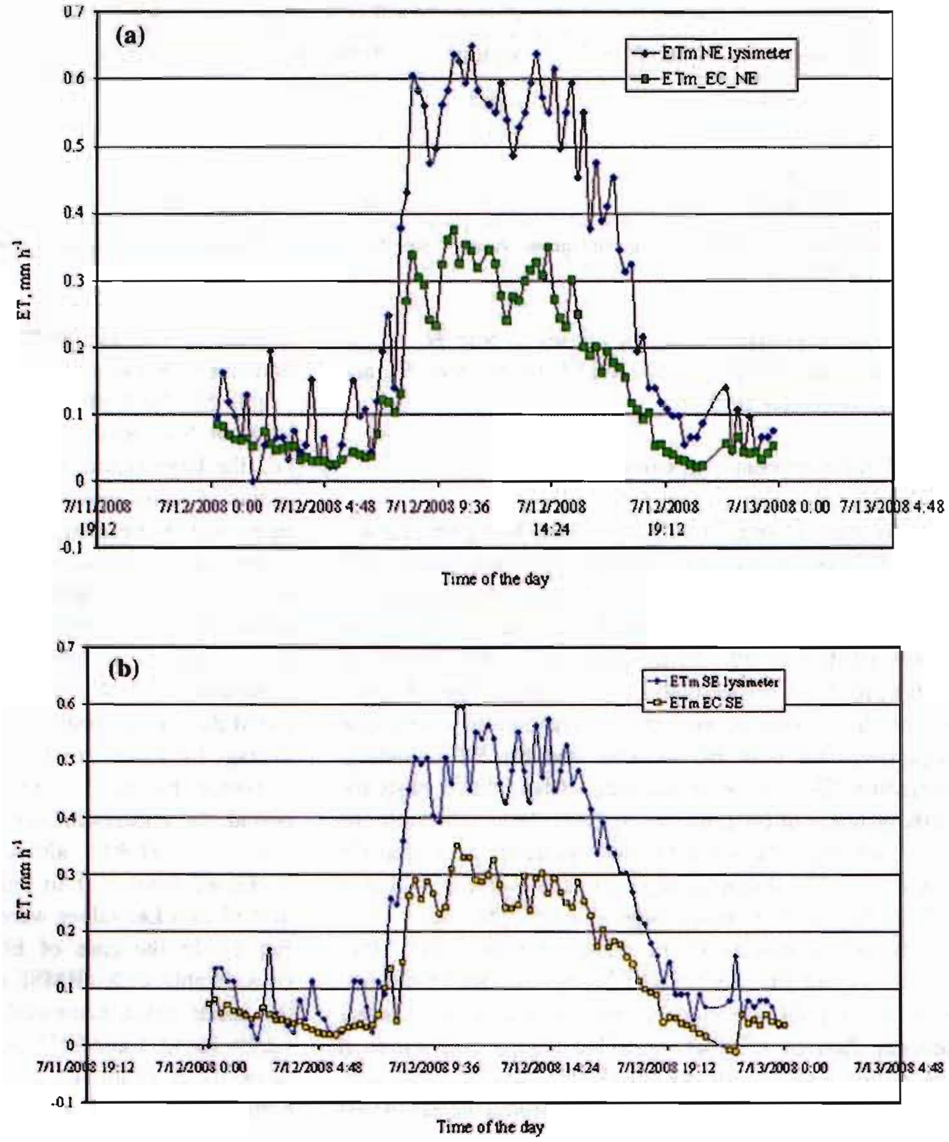


**Fig. 3** Diel eddy covariance (EC) and lysimeter ET (DOY 194) from northeast (NE) (**a**) and southeast (SE) (**b**) fields

(Table 7). However, after EB closure was forced on the daytime LE fluxes, the agreement with the lysimeter daytime ET remarkably improved, with a rather small bias and RMSE (Table 7). Still for the daytime ET analysis, the EC2 system in the south cotton field showed less error spread and a correlation line much closer to the 1:1 line (slope of 0.99 and intercept of almost 0).

These results, as in the previous case of *H*, show that LE (ET) was better measured by the EC system during the daylight hours. This fact is most probably due to the presence of increasing turbulent fluxes with the heating of the surface as the day progresses.

Composite ET for sites EC1 and EC2 resulted with an MBE ± RMSE value of −4.2 ± 17.7% and −9.7 ± 9.3%, respectively (Table 7). Although, most of the error, −33.8 ± 21.6% for EC1 and −11.4 ± 10.3% for EC2, occurred at ET values less than 3 mm $day^{-1}$ (note that the maximum ET value was 10 mm $day^{-1}$ at the north field, during DOY 208). Hence for ET values greater than 3 mm $day^{-1}$, EC-based composite ET agreed better with the lysimeter values, i.e., MBE ± RMSE values of 0.1 ± 0.6 mm $day^{-1}$ (or 1.7 ± 9.1%) for EC1 and −0.6 ± 0.6 mm $day^{-1}$ (or −7.5 ± 7.9%) for EC2, respectively.

Furthermore, observing the MBE, slope, intercept, and coefficient of determination for ET composite (Table 7; Fig. 6) corresponding to both EC systems, it can be seen that in average EC2 underestimated more daily ET than EC1. To understand this difference we recurred to the footprint analysis.

According to the 1D footprint model of Gash (1986), 92% of the turbulent fluxes originated within a distance of

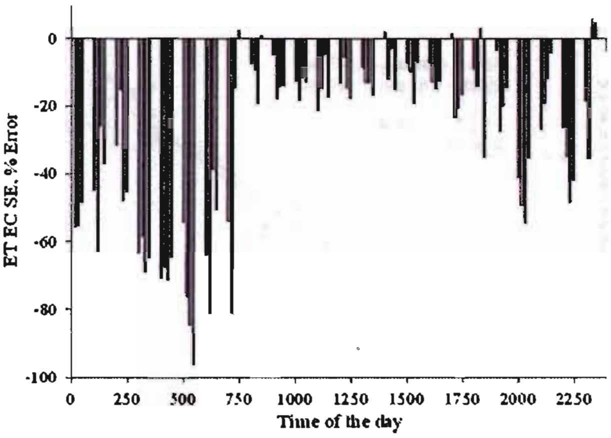


**Fig. 4** Larger southeast (SE) EC-based ET measurements errors (ET EC SE, %Error) occurred during nighttime, when the atmospheric condition tends to be stable to neutral and turbulence is very small or none

65–100 m upwind of the EC station. This FTP did not incorporate the atmospheric stability condition, thus actual FTP length may be somewhat longer. Gash's FTP relative and cumulative weights have been plotted along the upwind distance from the EC site in Fig. 7. Moreover, Schmid's (1994) 2D FTP, which uses the Monin–Obukhov similarity theory (Foken 2006) to account for atmospheric stability, predicted that 90% of the fluxes measured by the EC systems originated within a distance of 100–120 m upwind of the EC stations (Fig. 8). Complementing the previous two FTPs' results, Kaharabata et al. (1997) 2D FTP indicated that 97% of the heat fluxes originated within an upwind length of 200–280 m of the EC sites (FTP graph not shown). The latter two FTP models predicted that the leading edge of the 'flux source area' started about 10 m upwind of the EC systems. The FTP analysis was performed for a range of environmental conditions, i.e., unstable/stable atmospheric conditions, moderate to strong wind speeds (3.5–6.5 m $s^{-1}$), wind direction vector from the south to the west–southwest, different degrees of wind direction SD, ET rates, and crop heights (instrumentation height fixed at 2.5 m). These results indicate that the EC2 heat flux sensors, located at the south lysimeter field, potentially measured about 10% of fluxes that were generated in the fallow winter wheat (non-transpiring) field to the south, beyond the boundary of the southern cotton field.

Then, composite ET rates from the EC2 site were compensated (increased) proportionally (in percent) to FTP weights that lay outside of the cotton field. The FTP weights were probabilistically estimated by the weight FSAM (Schmid 1994). According to Chávez et al. (2005), the Schmid (1994) FSAM footprint better weighted/integrated heat fluxes estimated using airborne multispectral imagery and an aerodynamic temperature-based EB model, when compared to Kaharabata et al. (1997) FTP model and to arbitrary area of interest (AOI) polygons upwind of EC towers.

As a result of the FTP ET compensation, the EC2-based ET values matched the lysimetric ET values (Fig. 9) better. The error was relatively small, $-0.03 \pm 0.5$ mm $day^{-1}$ (or $-0.6 \pm 10.2\%$), with a correlation slope of 0.99, intercept of $-0.029$ and $R^2$ of 0.93. This result may be a strong indication that the EC-based composite ET values can be adjusted when LE is not entirely measured within the FTP area. In addition, the FTP model FSAM can be successfully applied to determine the extent of the source of heat fluxes and its relative weights to correctly represent the amount of fluxes originated from a given area within the FTP extent.

In the interpretation of how well the ET adjustment procedure improved EC-based ET, one must consider that the uncertainty in measured $G$ is around 15–20% and that for $R_n$ about 6–10%. Therefore, the AE may contribute to about 10% of errors; which roughly is in the same magnitude of error in EC-based ET after adjustments (e.g., composite ET plus FTP). Consequently, the procedures to adjust EC-based ET outlined in this study seem to adequately reproduce reference ET measured with precision large weighing lysimeters, in the advective/semi-arid climate of the Southern High Plains.

On the other hand, the EC1 system did not experience flux source area extent outside of the cotton fields, thus was not adjusted as in the EC2 case. However, the NE lysimeter cotton field ET was more than the SE field ET. The SE lysimeter in average measured $0.32 \pm 0.52$ mm $day^{-1}$ (or $-4.5 \pm 16.4\%$) less ET than the NE one from 1 April until

**Table 6** EC-based ET estimation errors when ET was obtained by averaging 15-min LE data over the entire day (24 h)

| Site | ET analysis | MBE (mm $day^{-1}$) | MBE (%) | RMSE (mm $day^{-1}$) | RMSE (%) | Slope | Intercept (mm $day^{-1}$) | $R^2$ |
|---|---|---|---|---|---|---|---|---|
| EC1 | No EB adjustment | −2.1 | −41.4 | 0.8 | 12.3 | 0.724 | −0.610 | 0.96 |
| EC2 | No EB adjustment | −2.0 | −34.1 | 0.7 | 7.4 | 0.669 | −0.052 | 0.92 |
| EC1 | EB closure forced | 0.3 | 1.0 | 0.8 | 19.3 | 1.190 | −0.786 | 0.95 |
| EC2 | EB closure | −0.7 | −12.0 | 0.6 | 10.1 | 0.807 | 0.393 | 0.89 |

*MBE* mean bias error, *RMSE* root mean squared error, $R^2$ coefficient of determination, *EC1* eddy covariance system 1, *EC2* eddy covariance system 2, *LE* latent heat flux, *EB* energy balance

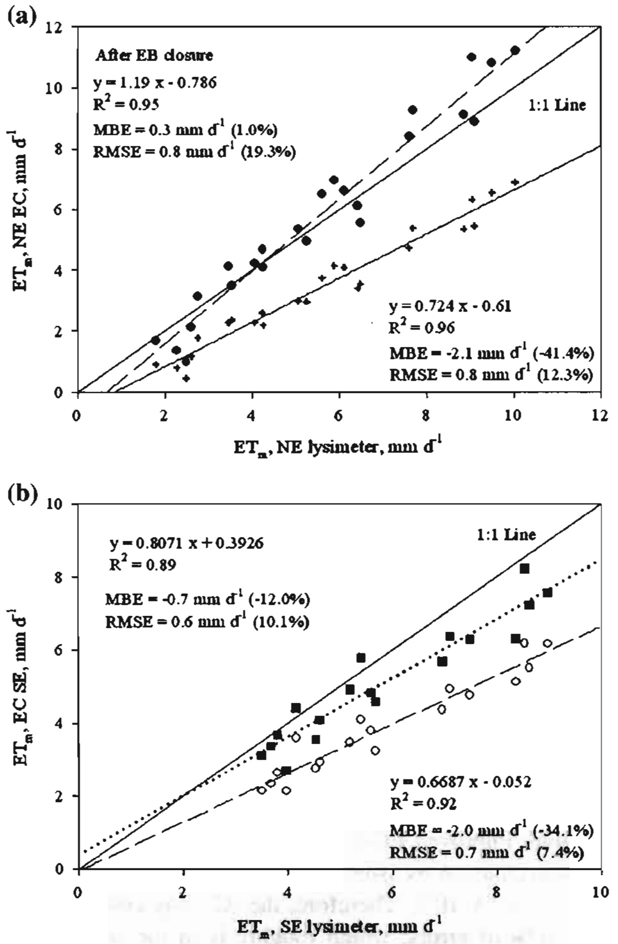


**Fig. 5** Eddy covariance (EC) versus lysimeter ET, 24 h ET with (*solid symbols*) and without (*plus sign* and *empty circle symbols*) EB closure, **a** Northeast (NE), **b** Southeast (SE) lysimeter field, respectively

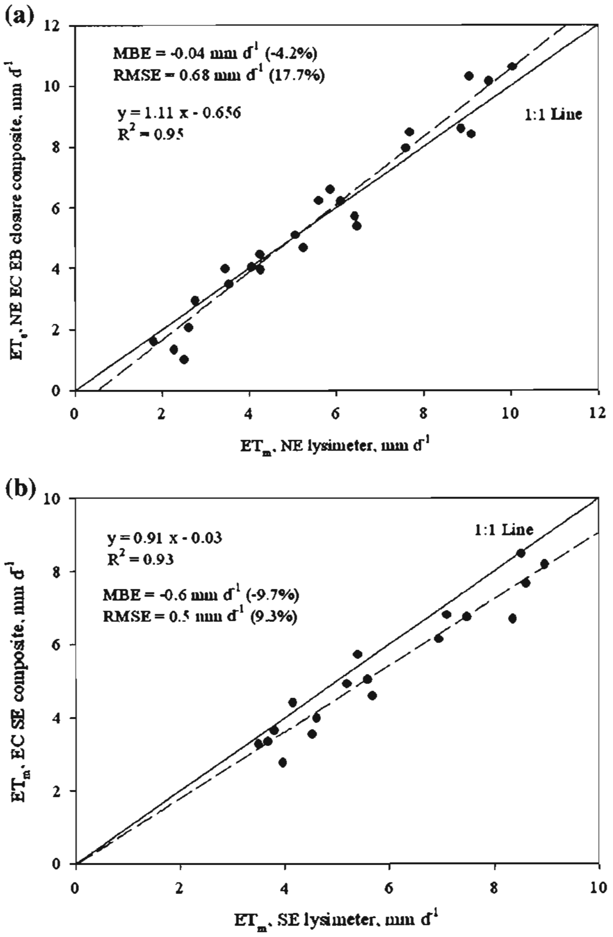


**Fig. 6** Northeast (NE) **a** eddy covariance system 1 (EC1) and southeast (SE), **b** eddy covariance system 2 (EC2) composite ET evaluation

mid-August. The lysimeter linear correlation (*X*-axis NE lysimeter, *Y*-axis SE lysimeter) parameters were, slope of 0.88, intercept of 0.2 mm day$^{-1}$, and $R^2$ of 0.99. These lower ET rates at the SE cotton field could have been associated with local or regional advection and/or crop row orientation. Colaizzi (2008) found greater radiation interception for N–S oriented rows than E–W oriented rows likely leading to slightly greater ET. Spatial variability of surface fluxes and surface soil moisture can occur within short distances of small fields. The NE field had N–S row orientation with greater solar irradiance interception while the SE field had E–W row orientation. Davenport and Hudson (1967) measured evaporation rates from open-

**Table 7** EC-based ET when computed using average daytime (~14 h) LE data

| Site | ET analysis | MBE (mm day$^{-1}$) | MBE (%) | RMSE (mm day$^{-1}$) | RMSE (%) | Slope | Intercept (mm day$^{-1}$) | $R^2$ |
|---|---|---|---|---|---|---|---|---|
| EC1 | No EB adjustment | −1.4 | −28.8 | 1.00 | 12.4 | 0.65 | 0.160 | 0.95 |
| EC2 | No EB adjustment | −1.3 | −26.0 | 0.50 | 8.2 | 0.78 | −0.203 | 0.95 |
| EC1 | EB closure forced | 0.03 | 6.2 | 0.54 | 17.6 | 0.88 | 0.570 | 0.96 |
| EC2 | EB closure forced | −0.1 | −12.3 | 0.40 | 8.4 | 0.99 | 0.040 | 0.94 |
| EC1 | Composite ET | −0.04 | −4.2 | 0.68 | 17.7 | 1.11 | −0.656 | 0.95 |
| EC2 | Composite ET | −0.6 | −9.7 | 0.50 | 9.3 | 0.91 | −0.030 | 0.93 |

*ET* evapotranspiration, *MBE* mean bias error, *RMSE* root mean squared error, $R^2$ coefficient of determination, *EC1* eddy covariance system 1, *EC2* eddy covariance system 2, *LE* latent heat flux, *EB* is energy balance

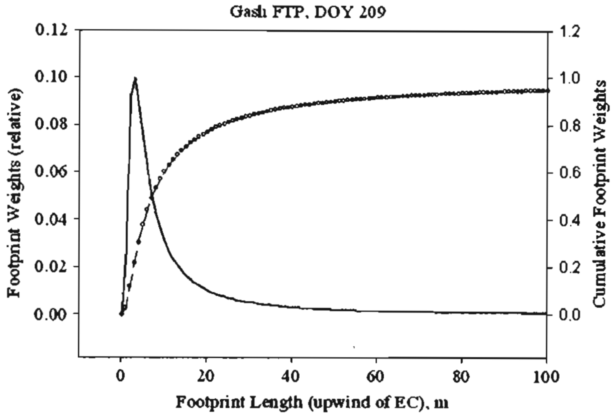


**Fig. 7** 1D Gash (1986) footprint showing 94.8% of the fetch at 110 m from the eddy covariance (EC) location for day of year (DOY) 209; considering neutral atmospheric conditions

water using evaporimeter dishes situated at the crop height and found the largest decrease in evaporation of about 30% within the first 60 m from the upwind of the cotton field into the interior. Burman et al. (1975) took climatic measurements along a 50-km transect from a dry sagebrush into the center of an irrigated field and found a 20% decline in evaporation. We believe the row orientation was the larger influence based on canopy radiation models (Colaizzi 2008) built upon Campbell and Norman (1998), and that the LE fluxes and ET rate differences as influenced by row orientation were important and often neglected in ET research.

Consequently, to evaluate how well the EC1-based ET measurements represented ET rates from the southeast, EC1 composite ET values were compared to values from the SE lysimeter field. This evaluation was performed considering that both cotton fields were similar (crop variety, development stage, water received, homogeneous canopy cover, etc.), only differing in the raw orientation, and also considering that some of the heat fluxes (eddies) recorded by EC1 might have come from the SE field (statistical footprint extent). This comparison indicted that the average difference was 0.82 mm day$^{-1}$ (13.5%), with a SD 0.58 mm day$^{-1}$ (8.4%). The linear regression between the EC1 composite ET values an SE lysimeter values also showed the larger EC1-based ET measurements with a correlation slope of 1.18, intercept of −0.225, and coefficient of determination of 96%. These results may indicate that the composite EC1-based ET values mainly represent cotton ET from the North field.

A last evaluation of the EC systems was carried out, this time LE was not adjusted for lack of EB closure using the BR method but instead measured LE was discarded and a new LE was estimated as a residual of the EB, assuming $H$ was properly measured by the EC systems.

In this analysis, we found out that ET errors were larger than when the BR was used to adjust LE for lack of EB closure (Table 8). Also, the correlation slope was lower and the intercept higher. The analysis of these data indicates that it is more appropriate to adjust heat fluxes for

**Fig. 8** Schmid (1994) 3D FSAM footprint representation showing 90% of the fetch to an extent of 110 m from the eddy covariance (EC) site on day of year (DOY) 209

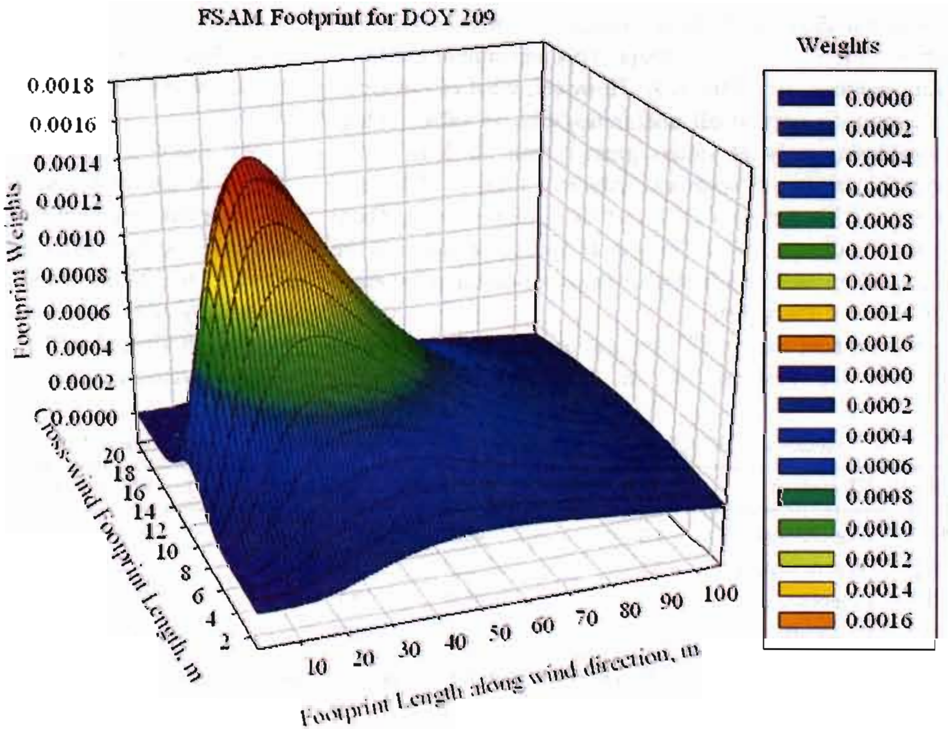

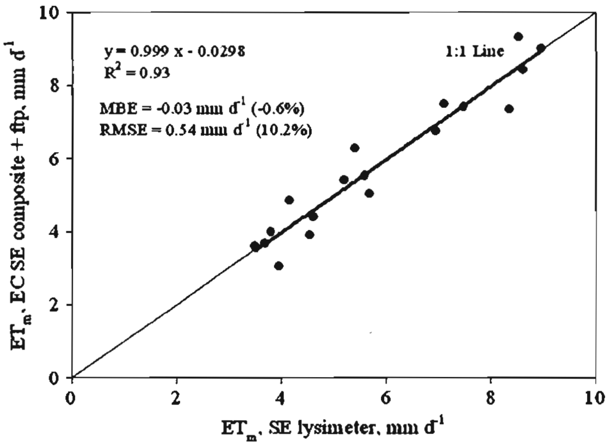


**Fig. 9** Eddy covariance system 2 (EC2) daily composite ET, including adjustments according to a heat source area/footprint (FTP) analysis

lack of EB closure using the BR method (with around-noon EC average BR values) instead of the EB residual method.

## Conclusions

Sensible heat flux, originated from two irrigated cotton fields, was on average under measured by 36.0 ± 30.0% using the EC systems during the growing season of June and July 2008. Larger errors were from nighttime sensible heat fluxes which apparently were not accurately measured by the EC systems. Thus, EB closure was 'forced' on EC-measured daytime *H* fluxes using the around-noon BR/preservation of energy concept. This adjustment considerably reduced the MBE on *H*. However, most of the errors occurred on very small and/or negative *H* values. Then, considering only *H* values greater than 50 W $m^{-2}$, the average daytime *H* error was reduce to −4.6 ± 15.1% and 1.3 ± 13.2% for sites EC1 and EC2, respectively. These results indicate that EC-based *H* measurements can be adjusted for lack of EB closure using around-noon average EC-derived BR values.

Latent heat flux or ET was also greatly under measured by the EC systems. As in the case of *H*, greater discrepancies occurred during nighttime hours. Therefore, a methodology was applied to adjust/compensate EC-measured ET values using the BR preservation of energy concept, only daytime measured heat fluxes, actual hours of daylight, and nighttime ET estimation. After the adjustments, and considering only ET values greater than 3 mm $day^{-1}$, the EC-based composite ET much better agreed with lysimeter values (i.e., errors decreased to 1.7 ± 9.1% and −7.5 ± 7.9% for EC1 and EC2, respectively).

Furthermore for the EC2 system, one more step/adjustment was inserted. In this procedure, the 'composite (daytime + nighttime)' ET value was increased in average 10% according to relative heat flux contribution weights generated by the FSAM 'flux source area' (footprint) model. Therefore, as a result of the footprint ET compensation, the EC2-based ET values matched lysimetric ET values well, with a relatively small −0.6 ± 10.2% error. This result is an indication that the EC-based composite ET values can be adjusted when LE is not entirely measured within the footprint area.

Considering that the uncertainty in measured *G* is around 20–30% and about 5–10% for $R_n$, the AE may contribute to about 10% of errors. Consequently, the procedures to adjust EC-based ET outlined in this study seemed to have adequately reproduced irrigated cotton ET measured with precision large weighing lysimeters, in the advective/semi-arid climate of the Southern High Plains.

In addition, it was shown that estimating ET as a residual of the EB, assuming that the sensible heat flux was correctly measured by the EC system, is not an adequate procedure and instead the BR method should be adopted to force EB closure on EC-measured sensible and latent heat fluxes.

As found in the literature, there are many potential causes of underestimation of sensible and latent fluxes by EC systems. We plan to explore some of them next, e.g., increase the high frequency flux sample averaging period from 15 to 30 min, 1 and 2 h to see whether different size/frequency eddies can be captured, provided diurnal trends can be avoided; as well as to study the effect of coordinates rotation/transformation on measured fluxes.

**Table 8** Evaluation of EC ET when computed using average daytime LE from the EB residual (LE = $R_n - G - H$)

| Site | ET analysis | MBE (mm $day^{-1}$) | MBE (%) | RMSE (mm $day^{-1}$) | RMSE (%) | Slope | Intercept (mm $day^{-1}$) | $R^2$ |
|---|---|---|---|---|---|---|---|---|
| EC1 | Avg. daytime ET | 1.8 | 45.1 | 0.7 | 36.0 | 0.85 | 2.70 | 0.93 |
| EC2 | Avg. daytime ET | −0.1 | 3.3 | 1.0 | 17.8 | 0.85 | 2.69 | 0.93 |
| EC1 | Composite | 1.1 | 27.4 | 0.7 | 24.6 | 0.87 | 1.82 | 0.94 |
| EC2 | Composite | 0.22 | 7.1 | 0.7 | 14.9 | 0.72 | 1.89 | 0.90 |

*ET* evapotranspiration, $R_n$ net radiation, *G* soil heat flux, *LE* latent heat flux, *H* sensible heat flux (all in W $m^{-2}$), *MBE* mean bias error, *RMSE* root mean squared error, $R^2$ the coefficient of determination, *EC1* eddy covariance system 1, *EC2* eddy covariance system 2, *Avg.* average, *EB* energy balance

**Acknowledgments** The authors are very thankful to the following individuals who provided technical assistance: Dr. Dario Canelon (University of Minneapolis), Dr. Sasha Ivans (Campbell Sci. Inc., Logan, Utah), Dr. John Prueger (USDA-ARS, Nat'l Soil Tilth Laboratory, Ames, IA), and to many Technicians from the USDA-ARS, Conservation and Production Research Laboratory, Bushland, TX. We also extend our appreciation to anonymous reviewers who helped improve the quality of this article.

## Appendix

Conversion of daytime average LE fluxes into ET rate

$$ET = \left(\frac{3,600 \times N \times LE}{\lambda_{LE} \times \rho_w}\right) \quad (16)$$

where ET is evapotranspiration (mm $day^{-1}$) converted from daytime average EC-measured LE (W $m^{-2}$). $\lambda_{LE}$ is the latent heat of vaporization (MJ $kg^{-1}$), equal to (2.501–0.00236 $T_a$), being $T_a$ in °C units, and $\rho_w$ is water density ($\sim$1 Mg $m^{-3}$). The 3,600 is a time conversion of s $h^{-1}$; while the $N$ is the number of bright sunshine hours per day. $N$ is computed as follows:

$$N = \left(\frac{24}{\pi} \times \omega_s\right) \quad (17)$$

where $\omega_s$ is the sunset hour angle (radians), computed as:

$$\omega_s = \arccos[-\tan(\Gamma)\tan(\delta)] \quad (18)$$

where $\Gamma$ is the location latitude (radians) and $\delta$ is the solar declination angle (radians).

$$\delta = 0.409 \times \sin\left(\frac{2\pi \times DOY}{366} - 1.39\right) \quad (19)$$

where DOY is the day of the year and 366 is the number of days in a leap year. In our case, 2008 was a leap year; otherwise the number should be 365 for a regular year.

## References


Baldocchi D (1994) A comparative study of mass and energy exchange over a closed C3 (wheat) and an open C4 (corn) canopy: I. The partitioning of available energy into latent and sensible heat exchange. Agric For Meteorol 67:191–220

Birks HJB, Line JM, Juggins S, Stevenson AC, ter Braak CJF (1990) Diatoms and pH reconstruction. Philos Trans Roy Soc Lond Ser B 327:263–278

Boegh E, Thorsen M, Butts MB, Hansen S, Christiansen JS, Abrahamsen P, Hasager CB, Jensen NO, van der Keur P, Refsgaard JC, Schelde K, Soegaard H, Thomsen A (2004) Incorporating remote sensing data in physically based distributed agro-hydrological modeling. J Hydrol 287(1–4):279–299

Burba GG, Anderson DJ (2007) Introduction to the eddy covariance method: General guidelines and conventional workflow. LI-COR Biosciences, http://www.licor.com, 141 pp (accessed 10 April 2008)

Burman RD, Wright JL, Jensen ME (1975) Changes in climate and estimated evaporation across a large irrigated area in Idaho. Trans ASAE 18(6):1089–1093

Campbell GS, Norman JM (1998) An introduction to environmental biophysics, 2nd edn. Springer, New York, p 286

Chávez JL, Neale CMU (2003) Airborne remote sensing of evapotranspiration over riparian vegetation in the middle Rio Grande river. Report to the US Bureau of Reclamation

Chávez JL, Neale CMU, Hipps LE, Prueger JH, Kustas WP (2005) Comparing aircraft-based remotely sensed energy balance fluxes with eddy covariance tower data using heat flux source area functions. J Hydromet AMS 6(6):923–940. doi:10.1175/JHM467.1

Chávez JL, Gowda PH, Howell TA, Copeland KS (2007) Evaluating three evapotranspiration mapping algorithms with lysimetric data in the semi-arid Texas High Plains. In: Proceedings of the 28th annual international irrigation show. Irrigation Association CD-ROM, San Diego, 9–11 Dec. 2007, pp 268–283,

Colaizzi PD (2008) Personal communication. See http://www.cprl.ars.usda.gov/Wetting%20Front/WF_Vol10-No1.pdf, pp 12–17, accessed on 4 September 2008

Davenport DC, Hudson JP (1967) Changes in evaporation rates along a 17-km transect in the Sudan Gezira. Agric Meteorol 4:339–352

Field RT, Heiser M, Strebel DE (1994) Measurements of surface fluxes. The FIFE Information System. 9 April 1994. Available at: http://www.esm.versar.com/FIFE/FIFEhome.htm http://www.esm.versar.com/FIFE/Summary/Sur_flux.htm. Accessed 10 September 2004

Fitzjarrald DR, Moore KE (1994) Growing season boundary layer climate and surface exchange in a subartic lichen woodland. J Geophys Res 99(D1):1899–1917

Foken T (2006) 50 Years of the Monin–Obukhov similarity theory. Boundary Layer Meteorol 119(3):431–447

Fritschen LJ, Qian P, Kanemasu ET, Nie D, Smith EA, Steward JB, Verma SB, Wesely ML (1992) Comparisons of surface flux measurement systems used in FIFE 1989. J Geophys Res 97(d17):18697–18713

Gash JHC (1986) A note on estimating the effect of a limited fetch on micrometeorological evaporation measurements. Boundary Layer Meterol 35:409–413

Hipps L (2003) Land–atmosphere interactions. Class notes and personal communication. Utah State University, PSB Department, Logan

Hipps L, Kustas WP (2001) Patterns and organization in evaporation. In: Grayson R, Bloschl G (eds) Spatial patterns in catchment hydrology: observations and modelling, Cambridge University Press, UK, pp 105–122. ISBN 0-521-63316-8

Holifield CD, Emmerich WE, Moran MS, Hernandez M, Scott RL, Bryant RB, King DM, Verdugo CL (2008) A remote sensing approach for estimating distributed daily net carbon dioxide flux in semiarid grasslands. Water Resour Res 44:W05S17. doi:10.1029/2006/WR005699

Horst TW, Weil JC (1992) Footprint estimation for scalar flux measurements in the atmospheric surface layer. Boundary Layer Meteorol 59:279–296

Horst TW, Weil JC (1994) How far is far enough? The Fetch requirement for micrometeorological measurement of surface fluxes. J Atmos Ocean Tech 11(4):1018–1025

Howell TA, Schneider AD, Dusek DA, Marek TH, Steiner JL (1995) Calibration and scale performance of Bushland weighing lysimeters. Trans ASAE 38:1019–1024

Kaharabata SK, Schuepp PH, Ogunjemiyo S, Shen S, Leclerc MY, Desjardins RL, MacPherson JI (1997) Footprint considerations in BOREAS. J Geophys Res 102(D24):29,113–29124

Kustas WP, Perry EM, Doraiswamy PC, Moran MS (1994) Using satellite remote sensing to extrapolate evapotranspiration

estimates in time and space over a semiarid Rangeland basin. Remote Sens Environ 49(3):275–286
Kustas WP, Hatfield JL, Prueger JH (2005) The soil moisture-atmosphere coupling experiment (SMACEX): background, hydrometeorological conditions and preliminary findings. J Hydromet AMS 6:791–804
Leclerc MY, Thurtell GW (1990) Footprint prediction of scalar fluxes using a Markovian analysis. Boundary Layer Meteorol 52:247–258
Leuning R (2007) The correct form of the Webb, Pearman and Leuning equation for eddy fluxes of trace gases in steady and non-steady, horizontal homogeneous flow. Boundary Layer Meteorol 123:263–267
Mahrt L (1998) Flux sampling error for aircrafts and towers. J Atmos Oceanic Technol 15:416–429
Malek E, Bingham GE (1993) Comparison of the Bowen ratio-energy balance and the water balance methods for the measurement of evapotranspiration. J Hydrol 146:209–220
Marek TH, Schneider AD, Howell TA, Ebeling LL (1988) Design and installation of large weighing monolithic lysimeters. Trans ASAE 31:477–484
Mauder M, Foken T (2006) Impact of post-field data processing on eddy covariance flux estimates and energy balance closure. Meterologische Zeitschrift 15(6):597–609
Mecikalski JR, Diak GR, Anderson MC, Norman JM (1999) Estimating fluxes on continental scales using remotely sensed data in an atmospheric-land exchange model. J Appl Meteorol 38:1352–1369
Moore CJ (1986) Frequency response corrections for eddy correlation systems. Boundary Layer Meteorol 37:17–35
Mu Q, Heinsch FA, Zhao M, Running SW (2007) Development of a global evapotranspiration algorithm based on MODIS and global meteorological data. Remote Sens Environ 111(4):519–536
New LL (2005) Agri-Partner irrigation result demonstrations 2005. Texas Cooperative Extension Service, Texas A&M University. Available on line at: http://amarillo.tamu.edu/programs/agripartners/irrigation2005.htm
Oncley SP, Foken T, Vogt R, Bernhofer C, Liu H, Sorbjan Z, Pitacco A, Grantz D, Ribeiro L (2000) The EBEX 2000 field experiment. In: 14th Symposium on boundary layers and turbulence. American Meteorological Society, Boston, Aspen, pp 322–324
Santos C, Lorite IJ, Tasumi M, Allen RG, Fereres E (2008) Integrating satellite-based evapotranspiration with simulation models for irrigation management at the scheme level. Irrig Sci 26:277–288. doi:10.1007/s00271-007-0093-9
Schmid HP (1994) Source areas for scalars and scalar fluxes. Boundary Layer Meteorol 67:293–318
Shuttleworth WJ (2007) Putting the "vap" into evaporation. Hydrol Earth Syst Sci 11(1):210–244
Suleiman A, Crago R (2004) Hourly and daytime ET from grassland using radiometric surface temperatures. Agron J 96:384–390
Todd RW, Evett SR, Howell TA (2000) The Bowen ratio-energy balance method for estimating latent heat flux of irrigated alfalfa evaluated in a semi-arid, advective environment. Agric For Meteorol 103(4):335–348
Tolk JA, Howell TA, Evett SR (2006a) Nighttime evapotranspiration from alfalfa and cotton in a semiarid climate. Agron J 98:730–736
Tolk JA, Evett SR, Howell TA (2006b) Advection influences on evapotranspiration of alfalfa in a semiarid climate". Agron J 98:1646–1654
Twine TE, Kustas WP, Norman JM, Cook DR, Houser PR, Meyers TP, Prueger JH, Starks PJ, Wesely ML (2000) Correcting eddy-covariance flux underestimates over a grassland. Agric For Meteorol 103(3):229–317
Verma SB (1998) Flux footprint estimates affected by measurement height, surface roughness and thermal stability. http://snrsl.unl.edu/georgeb/footprint/fp-title.html. Accessed on 10 June 2004
Weaver HL (1990) Temperature and humidity flux-variance relations determined by one-dimensional eddy correlation. Boundary Layer Meteorol 53:77–91
Webb EK, Pearman GI, Leuning R (1980) Correlation of flux measurements for density effects due to heat and water vapour transfer. Quart J Roy Meteorol Soc 106:85–100
Wilson K, Goldstein A, Falge E, Aubinet M, Baldocchi D, Berbigier P, Bernhofer C, Ceulemans R, Dolman H, Field C, Grelle A, Ibrom A, Law BE, Kowalski A, Meyers T, Moncrieff J, Monson R, Oechel W, Tenhunen J, Valentini R, Verma S (2002) Energy balance closure at FLUXNET sites. Agric For Meteorol 113(2002):223–243